Angewandte Chemie
Eine Zeitschrift der Gesellschaft Deutscher Chemiker

Supporting Information

69451 Weinheim, Germany

A Designed Functional Metalloenzyme that Reduces O_2 to H_2O with Over One Thousand Turnovers**

*Kyle D. Miner, Arnab Mukherjee, Yi-Gui Gao, Eric L. Null, Igor D. Petrik, Xuan Zhao, Natasha Yeung, Howard Robinson, and Yi Lu**

anie_201201981_sm_miscellaneous_information.pdf

Materials and Methods

All chemicals, unless otherwise specified, were obtained from Sigma (St. Louis, MO) or Fisher Scientific (Hampton, NH).

Purification of Proteins

The F33Y and G65Y mutations were introduced into Cu_BMb using a protocol previously described[1] and confirmed by DNA sequencing at the Biotechnology Center of the University of Illinois. E-F33Y-Cu_BMb and E-G65Y-Cu_BMb were purified from inclusion bodies with a yield of ~20 mg/L using a protocol previously described[2] with the following changes: R/Z was calculated using A_{408}/A_{280} for F33Y-Cu_BMb, and A_{410}/A_{280} for E-G65Y-Cu_BMb; for E-G65Y-Cu_BMb and E-F33Y-Cu_BMb protein with an R/Z values of ≥ 3.5 and ≥ 4, respectively, were used. E-Cu_BMb was purified as previously described[1] using a modified protocol for WTswMb.

Crystallization of Cu_BMb and F33Y-Cu_BMb

E-Cu_BMb (2.2 mM) in 20 mM tris(hydroxymethyl)aminomethane (tris) pH 8 (pH adjusted H_2SO_4), was mixed 1:1 with well buffer (0.2 M sodium acetate, 0.1 M tris hydrochloride pH 8.5, with 30% polyethylene glycol 4000) using the hanging drop method, with 300 µL well buffer in the well of the crystallization tray.

E-F33Y-Cu_BMb (1.0 mM) in 100 mM tris pH 8, (pH adjusted H_2SO_4), was mixed 1:3 with well buffer (0.1 M sodium cacodylate pH 6.5, 0.2 M sodium acetate trihydrate with 30% w/v polyethylene glycol 8000) using the hanging drop method with 300 µL well buffer in the well of the crystallization tray.

For the copper containing structure of F33Y Cu_BMb, crystals obtained as described above were soaked with 10 eq $CuSO_4$ in a mixture of E-F33Y Cu_BMb and well buffer consistent with the original drop conditions to avoid dissolving the crystals and subsequently with 15eq potassium cyanide, in a mixture of E-F33Y-Cu_BMb and well buffer using pH 7.0 sodium cacodylate.

Diffraction Data Collection

The crystals were first soaked briefly in cryoprotectant (30 % polyethylene glycol 400) and were flash frozen in liquid nitrogen. The diffraction data sets summarized in Supplementary Table 2 were collected at the National Synchrotron Light Source beamlines X12B, X26C, X29A (Upton, NY) and were processed with HKL2000 software[3].

Crystal Structure Determination

The crystal structure was solved by the molecular replacement method using MOLREP[4] in the CCP4 Package[5]. Initial refinement was performed using X-plor[6] and SHELX'97[7]. For E-Cu_BMb structure position of H43 and H29 was rebuilt using the program O[8]. For the E-F33Y-Cu_BMb the position of Y33 was rebuilt using the program O. Final refinements of E-F33Y-Cu_BMb and Cu-F33Y-Cu_BMb were carried out with the aid of Refmac5[9] and Coot[10].

Computer Modeling of Proteins

Computer models for E-F33Y-Cu_BMb and E-G65Y-Cu_BMb were created using Visual Molecular Dynamics[11] (VMD) and NAMD[12] (Molecular Dynamics Simulator) as described previously[2] with the following changes: The obtained E-Cu_BMb structure was used as a starting crystal structure and non-heme metals were not introduced into the simulation.

UV-Visible Spectroscopy

All UV-visible spectra were taken using an Agilent 8453 spectrometer (Agilent Technologies, Santa Clara, CA) using the supplied Chemstation software and kinetics package. Ferric protein spectra were obtained by using a 2 mL solution of 6 µM protein in buffer, as isolated. Deoxy protein spectra were taken after addition of excess sodium dithionite, for unambiguous assignment. For oxy protein spectra, the protein was reduced using ascorbic acid (1000 eq) and *N*,*N*,*N'*,*N'*-Tetramethyl-*p*-phenylenediamine

dihydrochloride (TMPD) (100 eq) and oxygen was bubbled into solution to ensure a clean oxygen-bound spectra.

For kinetic spectra monitoring the effect of reduction, 2 mL of 6 μM protein in air-saturated 50 mM potassium phosphate pH 6 with catalase (0.12 mg/mL) in a cuvette (sealed with a septum, wrapped with parafilm, and with stirring under an argon headspace) was first collected to obtain a ferric protein spectra. Then ascorbic acid (1000 eq) and TMPD (100 eq) was added and spectra were taken over time period of 60 minutes.

For determination of heme degradation rate, 4 mL of 18 uM protein was reduced using ascorbic acid (1000 eq) and TMPD (100 eq) in 50 mM potassium phosphate pH 6, In the absence or presence of up to 2 eq $CuSO_4$ and with or without 2.2 μM catalase. After addition of reductant the cuvette was capped to minimize oxygen from the air diffusing into solution. The rate obtained was used to correct observed rates of oxygen consumption obtained in the presence of copper for loss of heme due to degradation.

Oxygen Consumption Rate and Turnover Studies using an Oxygen Electrode

Ascorbic acid (1000 eq) and TMPD (100 eq) were added to 500 μL of 18 μM protein in air saturated 50 mM potassium phosphate pH 6. We choose to study the protein at pH 6 because we found that the enzymatic activity is higher at lower pH, likely due to more availability of protons, which can play a significant role in O_2 reduction to water. Consumption of oxygen was monitored using an oxygen electrode (Oxytherm System, Hansatech Instruments Ltd., Norfolk, England) with data collected every 0.1 seconds or a YSI Model 53 oxygen meter equipped with a water-jacketed and stirred-glass measuring vessel (1.8mL volume) with data collection every 0.6 seconds. Rates were calculated taking the derivative of the oxygen concentration using a 30 s data window (300 points or 50 points). For data where catalase and SOD (Enzo Life Sciences International, Inc., Plymouth Meeting, PA) were used, 2.2 μM and 250 units (as defined by manufacturer) were added, respectively, before addition of reductant. The reaction of catalase and SOD with hydrogen peroxide and superoxide respectively should produce one equivalent oxygen per two equivalents of the respective ROS [13,14]. The maximum initial rate was reported after subtraction of the background rate from reductant only. 8000 eq of ascorbate and 800 eq of TMPD was used in optimized condition which showed highest activity for E-G65Y-Cu_BMb.

The rates of oxygen consumption leading to water and reactive oxygen species were calculated as follows – the rate with ROS scavengers was subtracted from the rate without. The difference in rate doubled was the rate of ROS production (1 eq. O_2 produced for 2 eq. ROS consumed). The rate of ROS production was subtracted from the total rate to obtain the rate of oxygen consumption producing water. Propagation of uncertainty was carried out throughout, assuming the uncertainties were not covariant.

Turnover studies were performed with the same starting conditions as the rate studies, except that the starting oxygen concentration was ~500 μM (~28 eq). Reductant was added and oxygen consumption was monitored until all oxygen was consumed. After the consumption of all oxygen, approximately 500 μM of oxygen was introduced into solution through adding oxygen gas into the head space of sealed chamber. This process was repeated until we reached the observed number of turnovers. The number of turnovers during the oxygen addition was not considered in calculation of turnovers. After every 4 cycles, ascorbic acid (~330 eq) and TMPD (~33 eq) was added to compensate for consumed reductant.

^{17}O Nuclear Magnetic Resonance

^{1}H decoupled ^{17}O NMR spectra were collected at 81.3 MHz on a Varian UNITY INOVA spectrometer with a 5 mm AutoTuneX probe. Temperature was held constant at 25 °C by an FTS Systems unit. Gradient shimming was performed and the water signal was referenced to 0 ppm. Samples were placed inside an Omni-Fit NMR tube from Wilmad LabGlass (Vineland, NJ). ^{17}O labeled (phenol-^{17}O 35 %) L-tyrosine (~ 380 mM in water) was sealed inside of a capillary and placed inside the Omni-Fit (gas tight) NMR tube, serving as an external standard against which the $H_2{}^{17}O$ signal could be monitored. An external standard was used instead of an internal standard due to the high pH requirement for solubility as well as eliminating any possible interference in the reaction. The L-tyrosine concentration used allowed

detection in a matter of minutes and overcame the small volume of the capillary as well as 35% labeling of L-tyrosine. *N,N,N′,N′*-Tetramethyl-*p*-phenylenediamine dihydrochloride (TMPD) and ascorbic acid was added to the protein solution resulting in a 500 µL volume sample at a concentration of 50 µM protein, 5 mM TMPD, and 50 mM ascorbic acid in 50 mM potassium phosphate pH 6. Without delay an initial spectrum was collected over a period of ten minutes followed by removal from the instrument, injection of 1 mL $^{17}O_2$ at roughly atmospheric pressure (Cambridge Isotope Laboratories, Inc., Andover, MA, 70.7% oxygen-17 content) into the Omni-Fit NMR tube, sealing of the port, inversion for 15 seconds to aid in oxygen saturation of the solution, and subsequent data collection. During data collection the tube was spun at 10Hz to aid in mixing. Time points were collected as appropriate. In between each time point the tube was removed from the instrument, inverted for 15 seconds, and replaced. Data were analyzed using MestReNova (Mestrelab Research, Santiago de Compostela, Spain). The area of the tyrosine signal was set to 1 for all spectra and the area of the water signal was recorded in relation to this value.

UV-Visible Electronic Absorption Studies

Native or wild type sperm whale myoglobin (WTswMb) was used as a control for all UV-vis experiments. The ferric [Fe(III)] form (i.e. metMb), which is similar to the resting state of HCO, displays a Soret band ~ 409 nm, and visible absorption bands ~ 500 nm and 632 nm in the UV-visible spectrum (Supplementary Fig. 5A, black line). Upon reduction of ferric-WTswMb, the Soret band shifted to 432 nm, and the visible bands merged to a single band at 556 nm, typical of a reduced ferrous [Fe(II)] heme protein, called deoxyMb (Supplementary Fig. 5A, red line). Exposure to oxygen shifted the Soret band of deoxyMb to 418 nm and split the visible absorption into two bands ~ 540 and 580 nm, indicating the formation of oxyMb (Supplementary Fig. 5A, blue line). These results are similar to those reported previously[15].

Determination of K_d for F33Y Cu_BMb and G65Y Cu_BMb for copper

E-F33Y-Cu_BMb and E-G65Y-Cu_BMb were titrated with increasing amounts of copper and monitored using UV-Visible spectroscopy using a previously described method[1] to determine K_d. The spectra were analyzed using the method described by Bidwai, A. et al.[16] The determined K_d for F33Y-Cu_BMb and G65Y-Cu_BMb are 2 µM and 100 µM respectively.

Investigation of Oxygen Consumption Activity with copper

To more thoroughly investigate the effect of copper on Cu_BMb, F33Y-Cu_BMb, and G65Y-Cu_BMb, oxygen consumption rate studies with up to 2 eq $CuSO_4$ were performed. Under these conditions, the observed rate increased relative to those in the absence of copper; however, upon repeating in the presence 2.2 µM catalase, the apparent rate was too low to assign the observed copper induced rate increase in the absence of catalase to an increased HCO-like activity. The increase is therefore due to increased ROS production by copper and excess reductant. Under these conditions there was also a copper dependent heme oxygenase activity similar to that reported at pH 8 previously. Therefore, the observed HCO activity rates were corrected for the amount of verdoheme produced from heme (Supplementary Table 4) as this would inactivate a population of the protein assayed.

Supplementary Figures

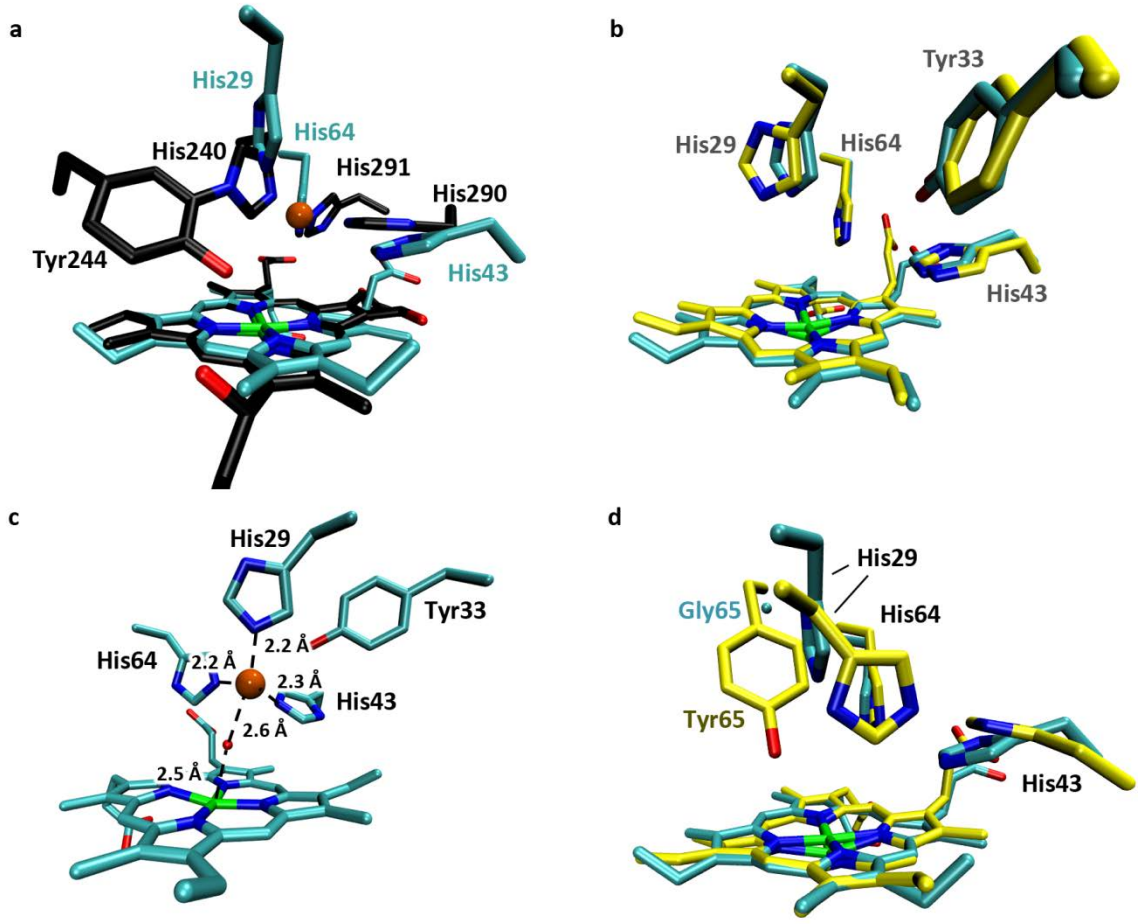

Figure S1. Additional Structures of Cu_BMb and Tyr containing mutants. (a) Overlay of the crystal structures of native bovine C*c*O[17] (black) and designed E-Cu_BMb (cyan); (b) Overlay of the computer model (yellow) and crystal structure (cyan) of E-F33Y-Cu_BMb. (c) Crystal structure of Cu-F33Y-Cu_BMb. Note: The distance between the copper (orange sphere) and the heme iron is 5.1 Å. (d) Overlay of E-Cu_BMb crystal structure (cyan) and the computer model of E-G65Y-Cu_BMb (yellow). Note: Gly65 is represented by the cyan sphere corresponding to the alpha carbon of Gly65

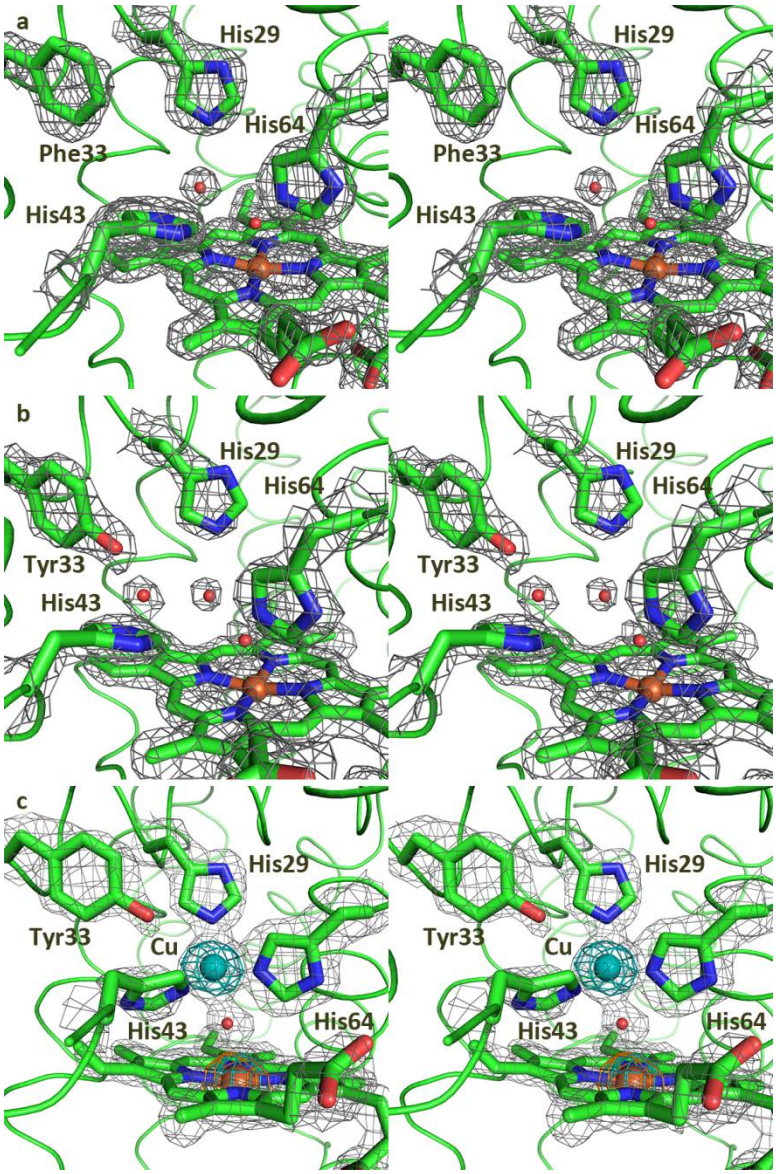

Figure S2. 2fo-fc electron density maps overlaid with presented crystal structures at a cutoff value of 1.3σ. (a) E-Cu_BMb (b) E-F33Y-Cu_BMb (c) Cu-F33Y-Cu_BMb. Anomalous density for Cu-F33Y-Cu_BMb below (1.3880 Å; orange) and above (1.372 Å; teal) Cu-K edge energy (1.3808 Å) at 5σ cutoff are shown in this panel (expected f" values at these wavelengths are 0.49 and 3.8 e for Cu and 2.7 e at both wavelengths for Fe). Note: Water over the heme iron in the E-Cu_BMb structure (a) was assigned based on density at lower cutoff. Maps were drawn in Pymol 1.3 from "O" map files generated in SHELXPRO (a) or ccp4 map files generated in ccp4 using FFT (b, c).

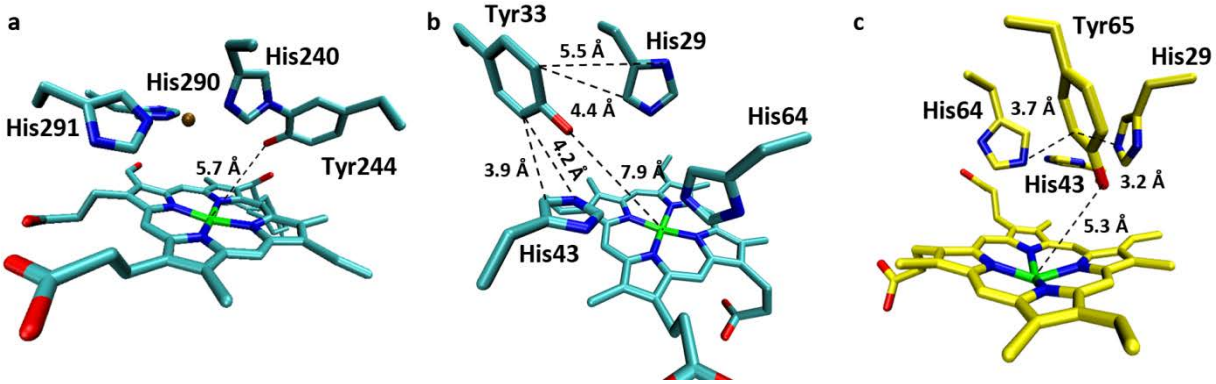

Figure S3. His-Tyr distances and Tyr-OH – heme Fe distances for (a) bovine CcO, (b) E-F33Y-Cu_BMb and (c) E-G65Y-Cu_BMb (model).

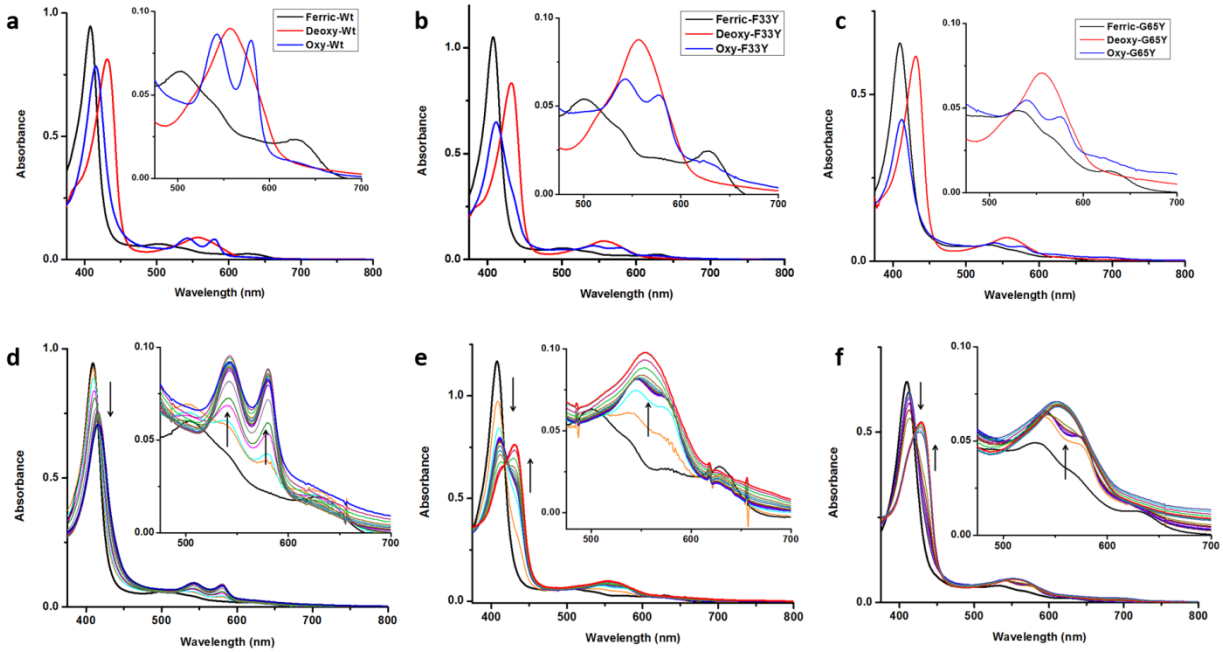

Figure S4. Reference spectra for ferric, oxy and deoxy forms of (a) WtswMb, (b) E-F33Y-Cu_BMb, and (c)E- G65Y-Cu_BMb Note: The feature at 540nm in (c) is due to a bis-His ligated population in the Ferric-E-G65Y Cu_BMb.[18,19]. UV-visible spectral changes of (d) ferric-WTswMb, (e) ferric-E-F33Y-Cu_BMb and (f) ferric-E-G65Y-Cu_BMb upon reduction with excess TMPD and ascorbate in air over 60 min.

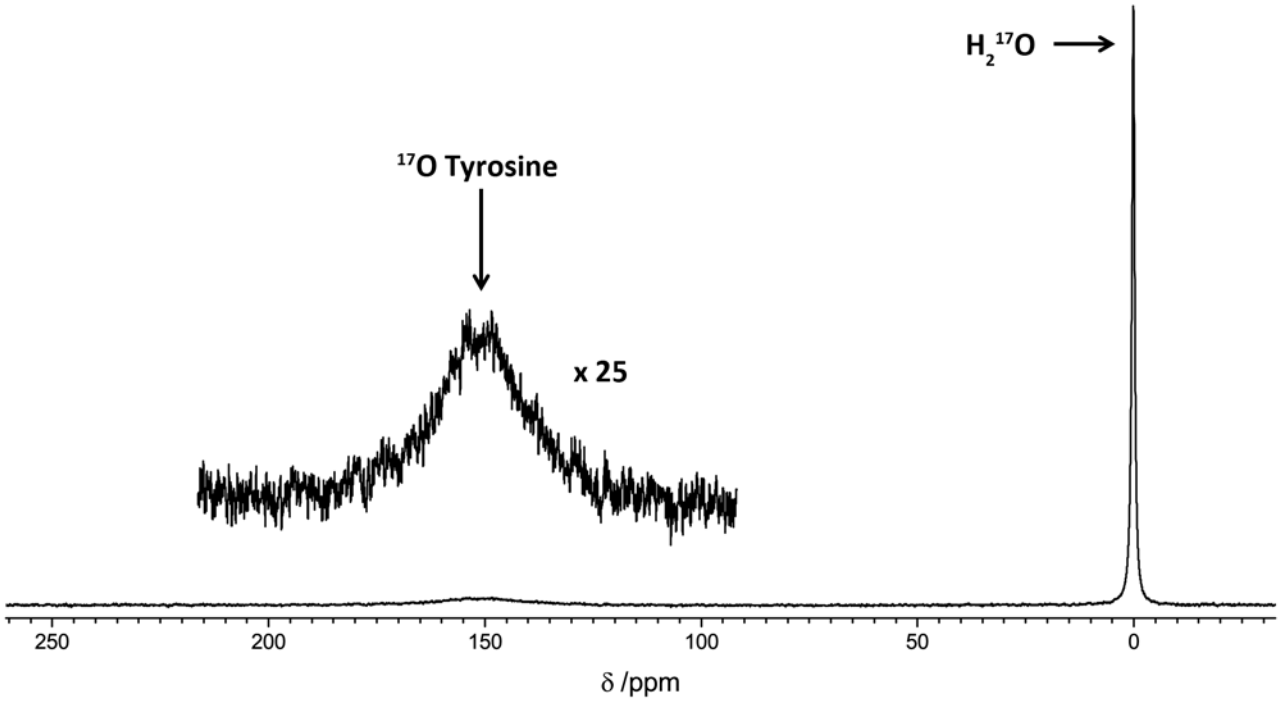

Figure S5. Typical ^{17}O NMR spectrum of the reaction of E-F33Y-Cu_BMb with $^{17}O_2$. ^{17}O Tyrosine peak scaled 25 times to show detail.

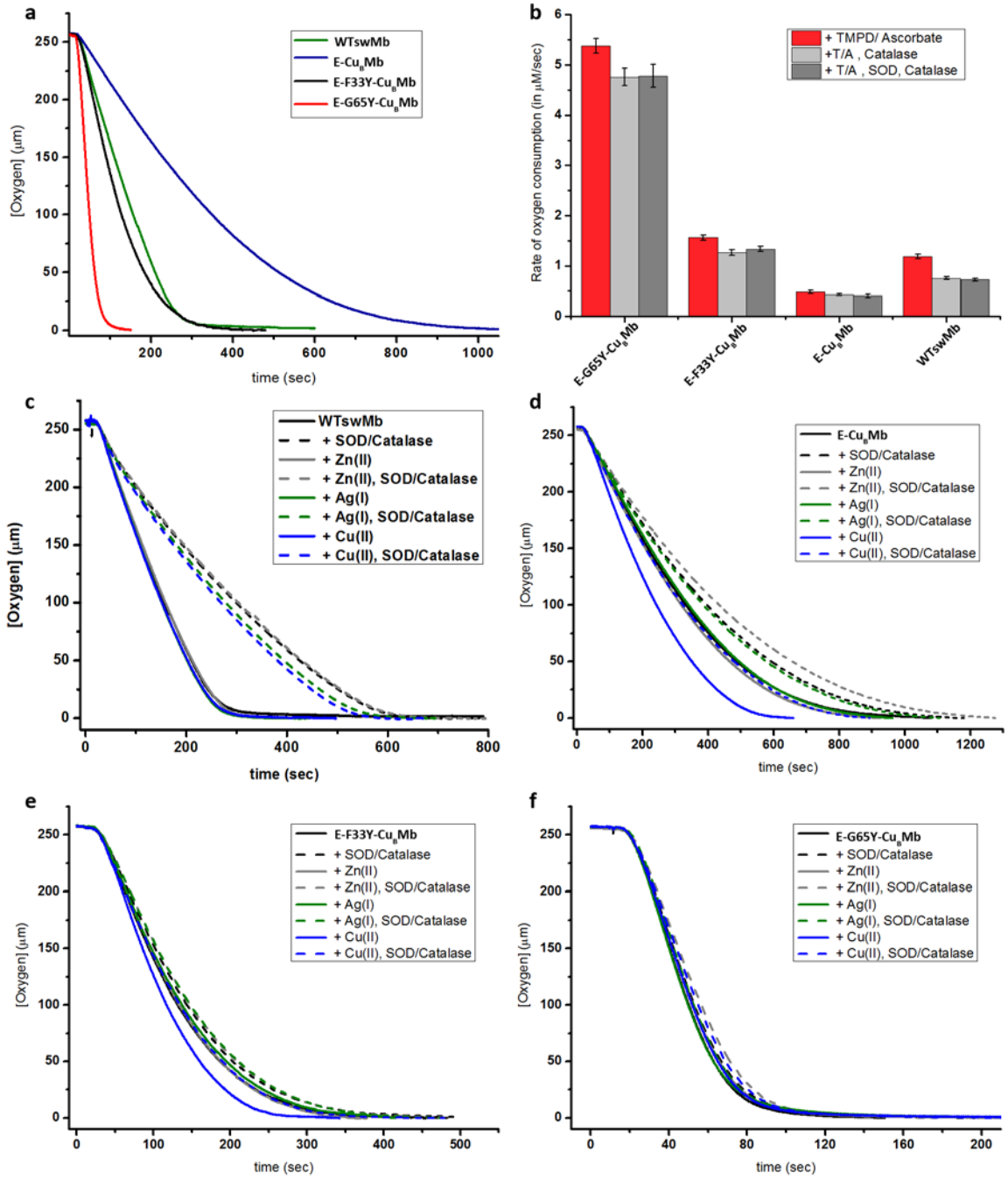

Figure S6. (a) Typical oxygen consumption traces for WTswMb (green), E-Cu$_B$Mb (blue), E-F33Y-Cu$_B$Mb (black), and E-G65Y-Cu$_B$Mb (red). (b) Oxygen consumption rates for all four proteins with and without SOD and catalase. (c) Typical oxygen consumption traces for WTswMb with and without SOD and catalase in the presence or absence of 1eq. Zn(II), Ag(I), or Cu(II). Typical oxygen consumption traces for (d) E-Cu$_B$Mb, (e) E-F33Y-Cu$_B$Mb and (f) E-G65Y-Cu$_B$Mb under the same conditions as (c). Note that the x-axes in (c) to (f) are plotted on different scales to clearly show small differences in the presence of metal ions. Error bars indicate standard deviation

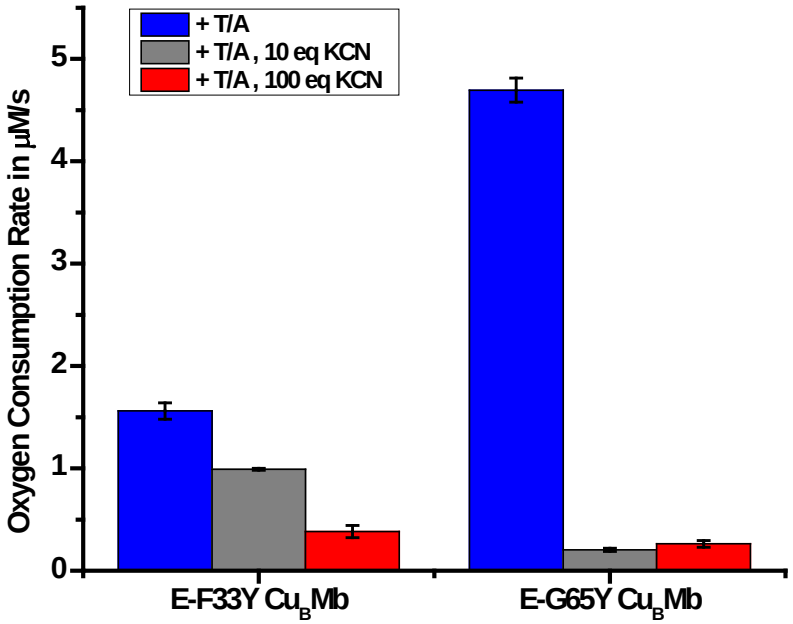

Figure S7. Effect of cyanide on E-F33Y-Cu_BMb and E-G65Y-Cu_BMb oxygen consumption activity. Error bars indicate standard deviation.

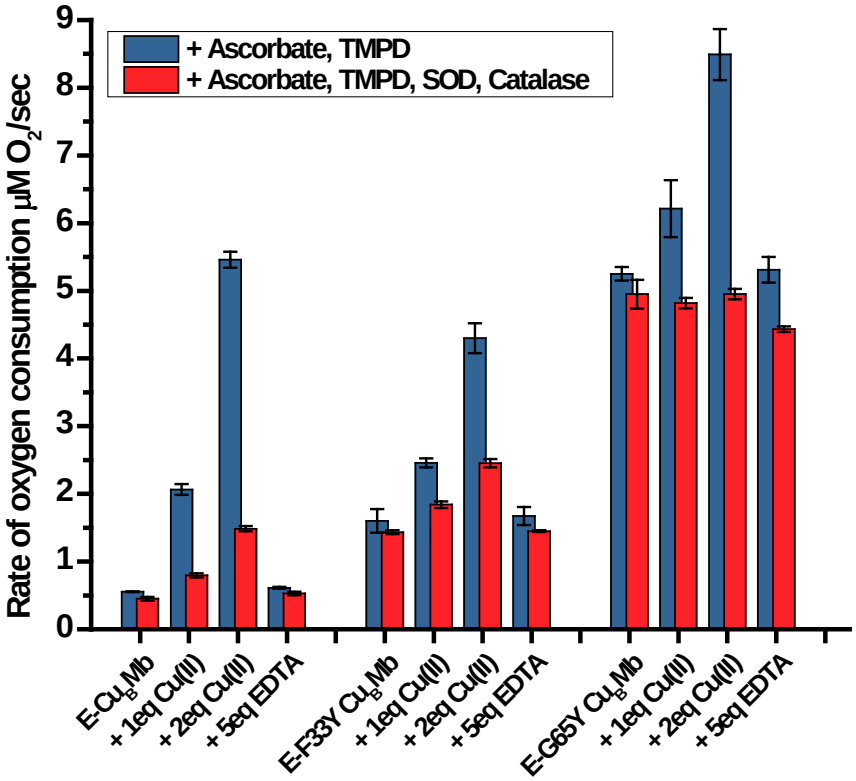

Figure S8. Oxygen consumption rates in the presence of EDTA and varying amounts of copper in the absence (Blue) or presence (Red) of catalase and SOD. Error bars indicate standard deviation.

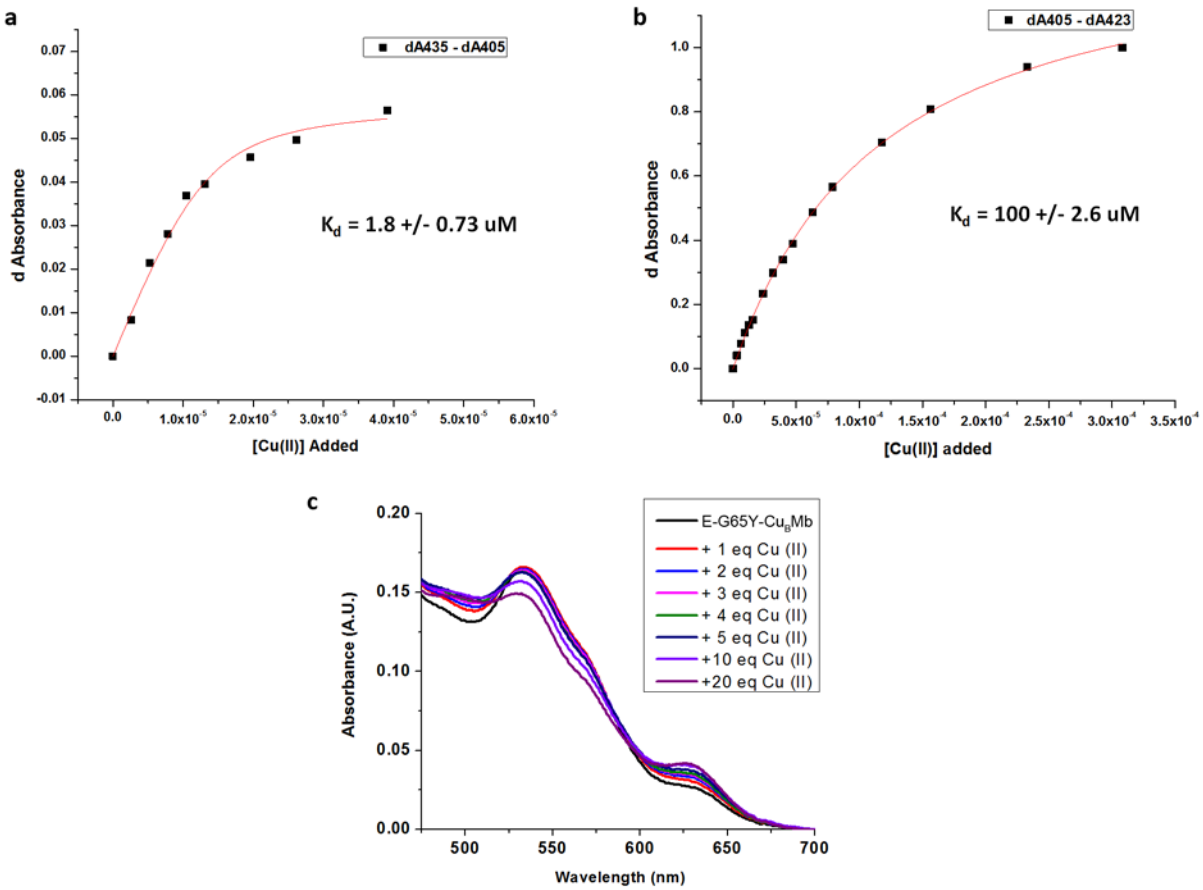

Figure S9. K_d values for F33Y-Cu$_B$Mb and G65Y-Cu$_B$Mb for copper. (a) Plot of difference in absorbance with increasing copper for F33Y-Cu$_B$Mb. (b) Same as (a) for G65Y-Cu$_B$Mb. (c) UV-spectra for G65Y-Cu$_B$Mb with copper showing changes with increasing copper.

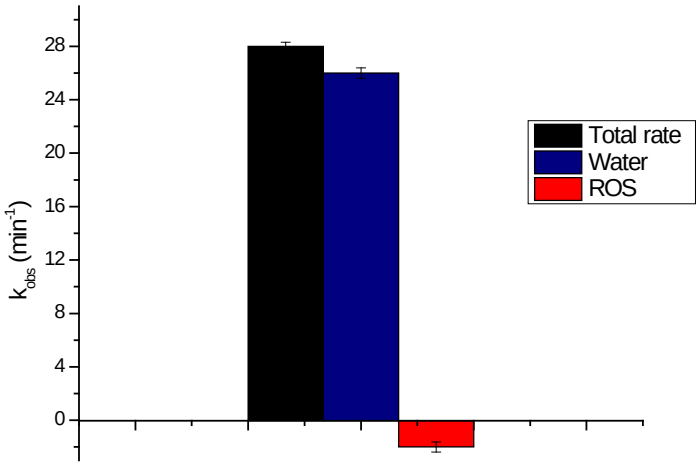

Figure S10. Oxygen consumption rate of E-G65Y-Cu$_B$Mb (6 μM) in the presence 8000 eq. ascorbate and 800 eq. TMPD. Error bars indicate standard deviation. k_{obs} indicates the rate constant under unsaturated condition both in terms of O_2 and reductant.

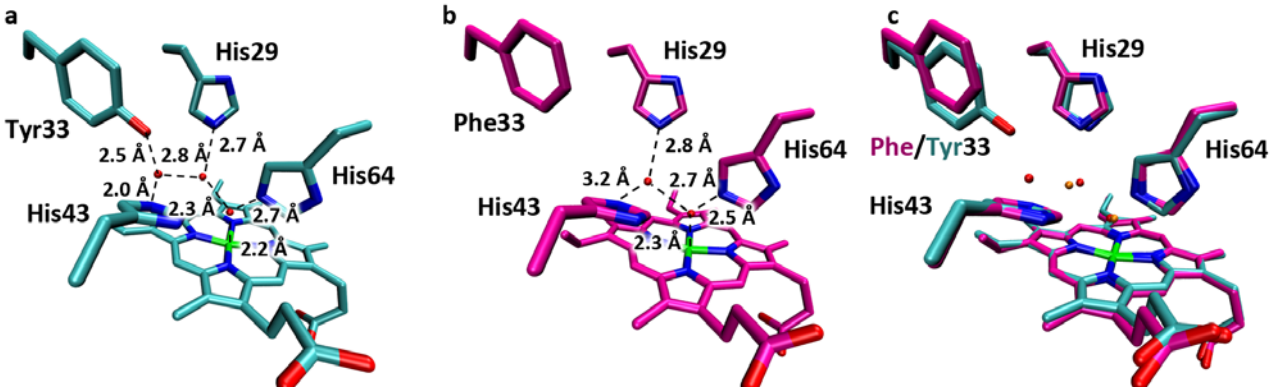

Figure S11. The water networks in the distal pockets of (a) E-F33Y-Cu_BMb and (b) E-Cu_BMb crystal structures. (c) Overlay of these structures (waters of Cu_BMb structure in orange).

Table S1 – ICP-MS results for levels of Ag, Cu, Fe, S, and Zn in as purified protein

	Concentration (ppm)					Ratio		
Sample	**Cu**	**Fe**	**S**	**Ag**	**Zn**	**Cu:Fe**	**Ag:Fe**	**Zn:Fe**
E-Cu_BMb	0.00	5.60	8.67	0.01	0.04	0.00	0.00	0.01
E-F33Y Cu_BMb	0.00	5.60	10.76	0.00	0.04	0.00	0.00	0.01
E-G65Y Cu_BMb	0.00	5.60	9.37	0.00	0.03	0.00	0.00	0.00

All samples were normalized to 5.60 ppm Fe for clearer comparison

Table S2 - Diffraction and refinement data for E-Cu_BMb, E-F33Y-Cu_BMb, and F33Y-Cu_BMb-Cu crystal structures

	E-Cu_BMb	E-F33Y-Cu_BMb	Cu-F33Y-Cu_BMb
Data collection			
Beamline	X12B	X26C	X29A
Wavelength (Å)	0.894	1.0000	1.0750
Space Group	$P2_12_12_1$	$P2_12_12_1$	$P2_12_12_1$
Cell dimension			
a, *b*, *c* (Å)	39.74, 47.68, 77.54	39.22, 47.72, 77.09	39.73, 48.29, 77.69
α, β, γ *(o)*	90.00, 90.00, 90.00	90.00, 90.00, 90.00	90.00, 90.00, 90.00
Resolution (Å)	1.90(1.97 – 1.90)	1.90(1.93 – 1.90)	1.80(1.86 – 1.80)
R-merge	0.065(0.347)	0.118(0.575)	0.111(0.637)
I/σI	40.1(9.8)	35.9(4.7)	23.3(4.6)
No. of Unique reflections	12,087	12,106	14,457
Completeness (%)	99.7(98.7)	99.4(100.0)	100.0(100.0)
Refinement			
Resolution (Å)	50.0– 1.90 (1.95-1.90)	50.0– 1.90 (1.95-1.90)	41.01– 1.80 (1.84-1.80)
Rwork/Rfree	0.204(0.245)/0.275(0.327)	0.210 (0.285)/0.266(0.429)	0.199(0.221)/0.247(0.331)
No. reflections	11,305	11,259	13,729
No. atoms			
Protein	1,218	1,219	1,218
Hem/Ion	42/1FE	42/1FE	42/1FE/1CU/4CU
Water	144	25	48
Metal Ion	Fe	Fe	Fe, Cu
B-factor			
Protein	23.4	29.9	34.0
HEM/Ion	18.4/18.2	25.1/24.5	34.5/27.1/38.41/61.6
Water	37.4	26.8	36.5
ESD(ESU)	0.017	0.131	0.097
Rms. deviations			
Bond lengths(Å)	0.006	0.018	0.019
Bond angles (°)	1.842	3.198	3.182

Table S3 – Data collection statistics for F33Y-Cu_BMb-Cu at above and below the copper K-edge (1.3808 Å).

	Cu-F33Y-Cu_BMb	
Data collection		
Wavelength (Å)	1.3880	1.3720
Space Group	$P2_12_12_1$	$P2_12_12_1$
Cell dimension		
a, b, c (Å)	39.68, 48.18, 77.48	39.69, 48.19, 77.51
α, *β, γ (o)*	90.00, 90.00, 90.00	90.00, 90.00, 90.00
Resolution (Å)	50-2.12(2.20-2.12)	50-2.12(2.20-2.12)
R-merge	0.094(0.584)	0.098(0.628)
I/σI	35.9(4.7)	23.3(4.6)
No. of Unique reflections	8,795	8976
Completeness (%)	100.0(99.9)	100.0(100.0)

Table S4 – Verdoheme formation rates (s^{-1}) in the absence and presence of catalase and SOD. Error indicated is standard deviation.

Reagents Added	E-Cu_BMb	E-F33Y Cu_BMb	E-G65Y Cu_BMb
+ 1 eq Cu^{2+}	8.47 $x10^{-3}$ ± 0.379 $x10^{-3}$	3.77 $x10^{-3}$ ± 0.130 $x10^{-3}$	8.83 $x10^{-3}$ ± 1.00 $x10^{-3}$
+ 2 eq Cu^{2+}	19.0 $x10^{-3}$ ± 0.812 $x10^{-3}$	7.91 $x10^{-3}$ ± 0.454 $x10^{-3}$	19.5 $x10^{-3}$ ± 0.790 $x10^{-3}$
+ 1 eq Cu^{2+}, Catalase, SOD	3.38 $x10^{-3}$ ± 0.409 $x10^{-3}$	2.07 $x10^{-3}$ ± 0.087 $x10^{-3}$	1.98 $x10^{-3}$ ± 0.117 $x10^{-3}$
+ 2 eq Cu^{2+}, Catalase, SOD	8.67 $x10^{-3}$ ± 1.24 $x10^{-3}$	5.78 $x10^{-3}$ ± 0.491 $x10^{-3}$	2.58 $x10^{-3}$ ± 0.322 $x10^{-3}$

Table S5 – Rates of oxygen reduction to form either water or superoxide/peroxide (ROS) with 18 µM WTswMb, Cu_BMb, F33Y-Cu_BMb, or G65Y-Cu_BMb, with and without metal.

	Rate of O2 consumption (µM s^{-1})		
	Total	To produce water	To produce ROS
WTswMb	1.18 ± 0.048	0.26 ± 0.068	0.9 ± 0.11
+ 1eq Zn(II)	1.16 ± 0.014	0.23 ± 0.055	0.93 ± 0.060
+ 1eq Ag(I)	1.19 ± 0.039	0.25 ± 0.080	0.9 ± 0.10
+ 1eq Cu(II)	1.26 ± 0.038	0.31 ± 0.058	0.95 ± 0.088
E-CuBMb	0.49 ± 0.035	0.33 ± 0.073	0.16 ± 0.095
+ 1eq Zn(II)	0.504 ± 0.0078	0.27 ± 0.048	0.24 ± 0.050
+ 1eq Ag(I)	0.45 ± 0.037	0.4 ± 0.13	0.1 ± 0.15
+ 1eq Cu(II)	0.75 ± 0.046	0.30 ± 0.071	0.5 ± 0.11
E-F33Y CuBMb	1.56 ± 0.055	1.1 ± 0.12	0.5 ± 0.15
+ 1eq Zn(II)	1.47 ± 0.067	1.09 ± 0.076	0.4 ± 0.14
+ 1eq Ag(I)	1.53 ± 0.058	1.0 ± 0.12	0.5 ± 0.16
+ 1eq Cu(II)	1.9 ± 0.11	0.9 ± 0.17	1.0 ± 0.26
E-G65Y CuBMb	5.4 ± 0.15	4.2 ± 0.49	1.2 ± 0.55
+ 1eq Zn(II)	4.9 ± 0.24	3.9 ± 0.25	1.0 ± 0.48
+ 1eq Ag(I)	5.2 ± 0.28	4.9 ± 0.38	0.3 ± 0.61
+ 1eq Cu(II)	5.02 ± 0.040	4.2 ± 0.11	0.9 ± 0.13

Table S6 – Relative concentration of $H_2{}^{17}O$ (normalized to initial concentrations) in reactions catalysed by WTswMb, E-F33Y-Cu_BMb, and E-G65Y-Cu_BMb.

	Relative concentration of $H_2{}^{17}O$			
	30 min	60 min	90 min	120 min
WTswMb	0.9 ± 0.12	0.86 ± 0.026	0.88 ± 0.027	0.99 ± 0.015
E-F33Y-Cu_BMb	1.14 ± 0.079	1.16 ± 0.050	1.25 ± 0.042	1.426 ± 0.0063
E-G65Y-Cu_BMb	1.2 ± 0.16	1.25 ± 0.071	1.4 ± 0.12	1.5 ± 0.19

References

(1) Sigman, J. A.; Kwok, B. C.; Lu, Y. *J. Am. Chem. Soc.* **2000**, *122*, 8192.
(2) Yeung, N.; Lin, Y.-W.; Gao, Y.-G.; Zhao, X.; Russell, B. S.; Lei, L.; Miner, K. D.; Robinson, H.; Lu, Y. *Nature* **2009**, *462*, 1079.
(3) Otwinowski, Z.; Minor, W. *Methods Enzymol.* **1997**, *276*, 307.
(4) Vagin, A.; Teplyakov, A. *J.Appl.Crystallogr.* **1997**, *30*, 1022.
(5) Bailey, S. *Acta Crystallogr.* **1994**, *D50*, 760.
(6) Brunger, A. T.; Adams, P. D.; Clore, G. M.; DeLano, W. L.; Gros, P.; Grosse-Kunstleve, R. W.; Jiang, J.-S.; Kuszewski, J.; Nilges, M.; Pannu, N. S.; Read, R. J.; Rice, L. M.; Simonson, T.; Warren, G. L. *Acta Crystallogr.* **1998**, *D54*, 905.
(7) Sheldrick, G. M.; Schneider, T. R. *Methods Enzymol.* **1997**, *277*, 319.
(8) Jones, T. A.; Zou, J. Y.; Cowan, S. W.; Kjeldgaard, M. *Acta Crystallogr.* **1991**, *A47*, 110.
(9) Vagin, A. A.; Steiner, R. A.; Lebedev, A. A.; Potterton, L.; McNicholas, S.; Long, F.; Murshudov, G. N. *Acta Crystallogr.* **2004**, *D60*, 2184.
(10) Emsley, P.; Cowtan, K. *Acta Crystallogr.* **2004**, *D60*, 2126.
(11) Humphrey, W.; Dalke, A.; Schulten, K. *J. Mol. Graphics* **1996**, *14*, 33.
(12) Phillips, J. C.; Braun, R.; Wang, W.; Gumbart, J.; Tajkhorshid, E.; Villa, E.; Chipot, C.; Skeel, R. D.; Kale, L.; Schulten, K. *J. Comput. Chem.* **2005**, *26*, 1781.
(13) McCord, J. M.; Fridovich, I. *J. Biol. Chem.* **1969**, *244*, 6049.
(14) Murthy, M. R. N.; Reid, T. J., III; Sicignano, A.; Tanaka, N.; Rossmann, M. G. *J. Mol. Biol.* **1981**, *152*, 465.
(15) Antonini, E.; Brunori, M.; Neuberger, A.; Tatum, E. L. *Hemoglobin and Myoglobin in their Reactions with Ligands*; Elsevier New York N. Y, 1971; Vol. 21.
(16) Bidwai, A.; Witt, M.; Foshay, M.; Vitello, L. B.; Satterlee, J. D.; Erman, J. E. *Biochemistry* **2003**, *42*, 10764.
(17) Tsukihara, T.; Shimokata, K.; Katayama, Y.; Shimada, H.; Muramoto, K.; Aoyama, H.; Mochizuki, M.; Shinzawa-itoh, K.; Yamashita, E.; Yao, M.; Ishimura, Y.; Yoshikawa, S. *Proc. Natl. Acad. Sci. U.S.A.* **2003**, *100*, 15304.
(18) Diven, W. F.; Goldsack, D. E.; Alberty, R. A. *J. Biol. Chem.* **1965**, *240*, 2437.
(19) Lin, Y.-W.; Yeung, N.; Gao, Y.-G.; Miner, K. D.; Lei, L.; Robinson, H.; Lu, Y. *J. Am. Chem. Soc.* **2010**, *132*, 9970.